



2-1999

The Arabidopsis *dwf/ste1* Mutant is Defective in the Δ^7 Sterol C-5 Desaturation Step Leading to Brassinosteroid Biosynthesis

Sunghwa Choe
University of Arizona


Takahiro Noguchi
RIKEN

Shozo Fujioka
RIKEN

Suguru Takatsuto
Joetsu University of Education

Christophe P. Tissier
University of Arizona

Follow this and additional works at: https://repository.upenn.edu/biology_papers
See next page for additional authors

 Part of the [Biology Commons](#), [Nucleic Acids, Nucleotides, and Nucleosides Commons](#), and the [Plant Breeding and Genetics Commons](#)

Recommended Citation

Choe, S., Noguchi, T., Fujioka, S., Takatsuto, S., Tissier, C. P., Gregory, B. D., Ross, A. S., Tanaka, A., Yoshida, S., Tax, F. E., & Feldmann, K. A. (1999). The Arabidopsis *dwf/ste1* Mutant is Defective in the Δ^7 Sterol C-5 Desaturation Step Leading to Brassinosteroid Biosynthesis. *The Plant Cell*, 11 (2), 207-221.
<http://dx.doi.org/10.1105/tpc.11.2.207>

At the time of this publication, Dr. Gregory was affiliated with the University of Arizona, but he is now a faculty member at the University of Pennsylvania.

This paper is posted at ScholarlyCommons. https://repository.upenn.edu/biology_papers/18
For more information, please contact repository@pobox.upenn.edu.

The Arabidopsis *dwf/ste1* Mutant is Defective in the Δ^7 Sterol C-5 Desaturation Step Leading to Brassinosteroid Biosynthesis

Abstract

Lesions in brassinosteroid (BR) biosynthetic genes result in characteristic dwarf phenotypes in plants. Understanding the regulation of BR biosynthesis demands continued isolation and characterization of mutants corresponding to the genes involved in BR biosynthesis. Here, we present analysis of a novel BR biosynthetic locus, *dwarf7* (*dwf7*). Feeding studies with BR biosynthetic intermediates and analysis of endogenous levels of BR and sterol biosynthetic intermediates indicate that the defective step in *dwf7-1* resides before the production of 24-methylenecholesterol in the sterol biosynthetic pathway. Furthermore, results from feeding studies with ^{13}C -labeled mevalonic acid and compactin show that the defective step is specifically the Δ^7 sterol C-5 desaturation, suggesting that *dwf7* is an allele of the previously cloned *STEROL1* (*STE1*) gene. Sequencing of the *STE1* locus in two *dwf7* mutants revealed premature stop codons in the first (*dwf7-2*) and the third (*dwf7-1*) exons. Thus, the reduction of BRs in *dwf7* is due to a shortage of substrate sterols and is the direct cause of the dwarf phenotype in *dwf7*.

Disciplines

Biology | Nucleic Acids, Nucleotides, and Nucleosides | Plant Breeding and Genetics

Comments

At the time of this publication, Dr. Gregory was affiliated with the University of Arizona, but he is now a faculty member at the University of Pennsylvania.

Author(s)

Sunghwa Choe, Takahiro Noguchi, Shozo Fujioka, Suguru Takatsuto, Christophe P. Tissier, Brian D. Gregory, Amanda S. Ross, Atsushi Tanaka, Shigeo Yoshida, Frans E. Tax, and Kenneth A. Feldmann

The Arabidopsis *dwf7/ste1* Mutant Is Defective in the Δ^7 Sterol C-5 Desaturation Step Leading to Brassinosteroid Biosynthesis

Sunghwa Choe,^a Takahiro Noguchi,^b Shozo Fujioka,^b Suguru Takatsuto,^c Christophe P. Tissier,^a Brian D. Gregory,^a Amanda S. Ross,^a Atsushi Tanaka,^{a,d} Shigeo Yoshida,^b Frans E. Tax,^a and Kenneth A. Feldmann^{a,1}

^aDepartment of Plant Sciences, University of Arizona, Tucson, Arizona 85721

^bInstitute of Physical and Chemical Research (RIKEN), Wako-shi, Saitama 351-0198, Japan

^cDepartment of Chemistry, Joetsu University of Education, Joetsu-shi, Niigata 943-8512, Japan

^dDepartment of Environment and Resources, Japan Atomic Energy Research Institute (JAERI), 1233 Watanuki-machi, Takasaki-shi, Gunma 370-1292, Japan

Lesions in brassinosteroid (BR) biosynthetic genes result in characteristic dwarf phenotypes in plants. Understanding the regulation of BR biosynthesis demands continued isolation and characterization of mutants corresponding to the genes involved in BR biosynthesis. Here, we present analysis of a novel BR biosynthetic locus, *dwarf7* (*dwf7*). Feeding studies with BR biosynthetic intermediates and analysis of endogenous levels of BR and sterol biosynthetic intermediates indicate that the defective step in *dwf7-1* resides before the production of 24-methylenecholesterol in the sterol biosynthetic pathway. Furthermore, results from feeding studies with ¹³C-labeled mevalonic acid and compactin show that the defective step is specifically the Δ^7 sterol C-5 desaturation, suggesting that *dwf7* is an allele of the previously cloned *STEROL1* (*STE1*) gene. Sequencing of the *STE1* locus in two *dwf7* mutants revealed premature stop codons in the first (*dwf7-2*) and the third (*dwf7-1*) exons. Thus, the reduction of BRs in *dwf7* is due to a shortage of substrate sterols and is the direct cause of the dwarf phenotype in *dwf7*.

INTRODUCTION

Sterols are known to play at least two critical roles in plants: as bulk components of membranes regulating stability and permeability (Bach and Benveniste, 1997) and as precursors of growth-promoting brassinosteroids (BRs; Fujioka and Sakurai, 1997). Sterol biosynthesis in plants has been studied extensively through enzyme purification or gene cloning (Grunwald, 1975; Goodwin, 1979; Benveniste, 1986; Bach and Benveniste, 1997). Figure 1 shows the proposed biosynthetic pathway from squalene to brassinolide (BL). A major difference between photosynthetic and nonphotosynthetic organisms is that cyclization of squalene 2,3-oxide is bifurcated to a different route for each system (Benveniste, 1986). In animals and yeast, squalene 2,3-oxide is cyclized to lanosterol, whereas in photosynthetic organisms it is cyclized to cycloartenol (Nes and McKean, 1977). Accordingly, photosynthetic organisms require somewhat different biosynthetic enzymes, such as cycloartenol synthase (Corey et al., 1993) and cycloeucalenol-obtusifolol isomerase, which are required to open the cyclopropane ring in cycloartenol

(Figure 1). However, most of the enzymatic steps are shared between the two different pathways.

In plants, sterols are subject to a series of modifications before conversion to BL. Different sterols, such as 24-methylenecholesterol (24-MC), campesterol (CR), isofucoesterol, and sitosterol, are converted to the BL congeners dolicholide, BL, 28-homodolicholide, and 28-homoBL, respectively, in a species-specific manner (Fujioka et al., 1995; Sasse, 1997). The BR-specific pathway diverges into the early and the late C-6 oxidation pathways. In the early C-6 oxidation pathway, introduction of a 6-oxo group occurs before the vicinal hydroxylation reactions at the side chain, whereas it occurs after these hydroxylations in the late C-6 oxidation pathway (Figure 1; Choi et al., 1997).

Several mutants, such as *constitutive photomorphogenesis* and *dwarfism* (*cpd*), *deetiolated2* (*det2*), and *dwarf4* (*dwf4*), have been shown to be defective in the BR-specific pathway (Li et al., 1996, 1997; Szekeres et al., 1996; Choe et al., 1998). These BR biosynthetic dwarfs share a characteristic dwarf phenotype, which includes short robust stems, reduced fertility, prolonged life cycle, and dark-green, round, and curled leaves when grown in the light. In the dark, these mutants exhibit short hypocotyls and expanded

¹To whom correspondence should be addressed. E-mail feldmann@ag.arizona.edu; fax 520-621-7186.

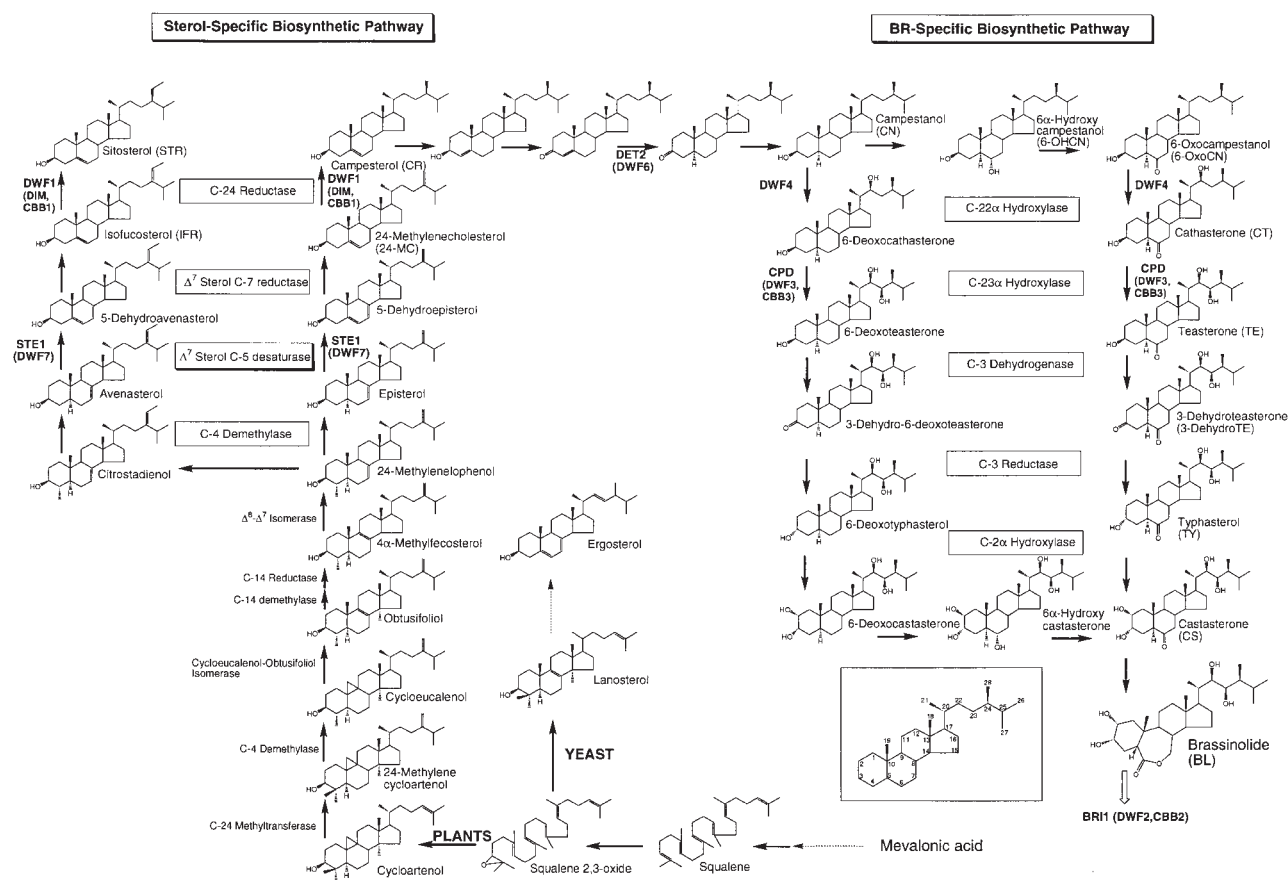


Figure 1. The Proposed BL Biosynthetic Pathway from Squalene to BL.

The BL biosynthetic pathway is divided into the sterol-specific pathway, squalene to campesterol, and the BR-specific pathway, campesterol to brassinolide. Common names for the compounds are labeled, and proposed enzymes involved in each reaction are boxed and labeled. Genes identified by mutants are marked. The acronyms for some compounds are in parentheses. In the inset, the carbon atoms of the sterol core rings and side chain are numbered.

cotyledons. *cpd* (*dwf3*) mutants are only rescued by 23 α -hydroxylated compounds (Szekeres et al., 1996). The *CPD* gene was shown to encode a cytochrome P450 steroid hydroxylating enzyme (CYP90A1). In addition, Li et al. (1996, 1997) showed that *det2/dwf6* is blocked in the C-5 reduction step. *DET2* was found to be homologous to steroid 5 α -reductases. Like its animal equivalents, *DET2* successfully converted progesterone (3-oxo- $\Delta^{4,5}$ steroid) to 4,5-dihydroprogesterone in a human cell line. In addition, the human 5 α -reductase gene effectively complemented *det2* mutants (Li et al., 1997). Recently, we have shown that *DWF4* encodes a cytochrome P450 whose amino acid sequence is 43% identical to *CPD*; *DWF4* has been named CYP90B1 (Choe et al., 1998). Based on results from feeding studies using BR biosynthetic intermediates, we showed that the proposed rate-limiting step of BR biosynthesis, 22 α -hydroxylation, is blocked in *dwf4* mutants.

In the plant sterol biosynthetic pathway, several of the genes have been cloned or identified based on heterologous expression or sequence similarity. First, Corey et al. (1993) isolated a cycloartenol synthase cDNA by heterologous complementation of yeast mutants lacking lanosterol synthase. In addition, two types of cDNAs encoding sterol methyltransferases have been isolated from soybean (Shi et al., 1996) and Arabidopsis (Husselstein et al., 1996). The Arabidopsis cDNA has been shown to mediate a second methyltransferase step leading to C₂₉ sterols (Bouvier-Navè et al., 1997). For the 14 α -demethylation reaction, Bak et al. (1997) cloned the cDNA encoding the 14 α -demethylase cytochrome P450 enzyme (CYP51) from *Sorghum bicolor*. Based on sequence similarity, Grebenok et al. (1997) identified an Arabidopsis sterol C-8 isomerase (GenBank accession number AF030357). Furthermore, an *ERGOSTEROL25* (*ERG25*) homolog for Arabidopsis (C-4 demethylase) also

has been discovered in the genome sequencing project (GenBank accession number AL021635). Finally, a sterol C-7 reductase has been cloned by heterologous expression of an Arabidopsis cDNA in yeast (Lecain et al., 1996).

As compared with the wealth of cloned genes in sterol biosynthesis, only one mutant has been found in these genes. Gachotte et al. (1995) screened an ethyl methane-sulfonate (EMS)-induced mutant population (22,000 M_2 plants) for mutants displaying an altered sterol profile. The screen yielded one mutant, *sterol1* (*ste1*), whose endogenous level of C-5-desaturated sterols is reduced to 30% of that of the wild type. Expression of the yeast gene *ERG3* (the gene for Δ^7 sterol C-5 desaturase) in the *ste1-1* mutant increased the level of C-5-desaturated sterols 1.7- to 2.8-fold compared with the *ste1-1* control, suggesting functional conservation of the enzymes from yeast and plants. However, visible phenotypes were not found in *ste1-1* plants. Thus, the authors hypothesized that the residual 30% level of C-5-desaturated sterols was sufficient for the growth of plants.

We have been characterizing a large collection of BR dwarf mutants. Of the eight *dwf* loci identified to date, *dwf3* (*cpd*; Szekeres et al., 1996), *dwf4* (Choe et al., 1998), and *dwf6* (*det2*; Li et al., 1996) have been shown to act in the BR biosynthetic pathway, whereas *dwf2* (*bri1*) probably is involved in BR perception (Clouse et al., 1996; Li and Chory, 1997). In this study, we provide a morphological and genetic characterization of *dwf7*. Based on our results from biochemical analyses, including feeding studies and quantification of endogenous levels of BRs, we hypothesize that *dwf7* mutants possess lesions in the *STE1* gene previously cloned by Gachotte et al. (1996). Here, we show that the *STE1* locus in *dwf7* mutants contains loss-of-function mutations, and we designate *dwf7-1* and *dwf7-2* as *ste1-2* and *ste1-3*, respectively.

RESULTS

Isolation of *dwf7* Mutants

The *dwf7-1* mutant originally was identified in a screen of 14,000 T-DNA-transformed lines of Arabidopsis. Genetic complementation tests with other *dwf* loci indicated that *dwf7* belongs to a unique complementation group. *dwf7-1* segregated as a monogenic recessive mutation; progeny from a heterozygote segregated 325 (wild type):98 (*dwf7-1*). Although *dwf7-1* originated from a T-DNA mutant population, it failed to cosegregate with the kanamycin resistance marker in the T-DNA, suggesting that *dwf7-1* was an untagged mutant. Furthermore, mapping the *dwf7-1* mutation to the Arabidopsis genome by using simple sequence length polymorphisms (SSLPs; Bell and Ecker, 1994) confirmed that *dwf7* maps to a location different from previously iso-

lated dwarfs. The meiotic recombination ratio between *dwf7* and the SSLP marker *nga172* on chromosome 3 was scored as 0/86, indicating tight linkage of *dwf7* to *nga172*. According to a recent recombinant inbred map of Arabidopsis, *nga172* is located 2.2 centimorgans from the top of chromosome 3.

A second allele of *dwf7* was identified among 43 dwarf mutants isolated by screening >50,000 M_2 seeds of an EMS mutant population. Similar to *dwf7-1*, the new allele was biochemically complemented by early BR biosynthetic intermediates, including 22 α -hydroxycampesterol (22-OHCR) and cathasterone (data not shown), and mapped near *nga172* (data not shown). Sequencing revealed a premature stop codon in exon 1 (see below).

Morphological Analysis of *dwf7-1*

dwf7 displays many of the characteristics of other BR dwarfs as shown in Figure 2. Compared with 1-month-old wild-type plants (Figure 2A), *dwf7-1* plants grown for 5 weeks in the light possess short robust inflorescences, dark-green, round leaves, reduced fertility, and short pedicels and siliques (Figure 2C). The wild type generally terminates flowering before 7 weeks of age; however, *dwf7-1* continues to produce flowers at this age, indicating a prolonged life span (Figure 2B). Additional morphological defects of 5-week-old light-grown plants are summarized in Table 1. Most noticeably, the height of *dwf7-1* plants is strikingly reduced and is only 14% that of wild-type height. The leaf blade width of *dwf7-1* mutants is similar to that of wild-type plants; however, the length is greatly reduced (1.8 cm) as compared with that of the wild type (3 cm), resulting in the round shape of *dwf7-1* leaves. The overall morphology of *dwf7-2* was similar to *dwf7-1* except that it was slightly shorter and more sterile (data not shown).

Because null mutations in the BR pathway result in a dwarf phenotype, as well as defects in skotomorphogenesis, we compared the *dwf7-1* mutant with other BR dwarfs for growth in the dark. Hypocotyl lengths from the longest to the shortest were 18 ± 1.6 (wild type; units in millimeters \pm SE; $n = 15$), 6.3 ± 0.29 (*dwf7-1*), 4.1 ± 0.03 (*det2/dwf6*), 1.26 ± 0.09 (*dwf4*), 1.24 ± 0.08 (*cpd/dwf3*), and 1.18 ± 0.08 (*bri1/dwf2*). These data indicate that *dwf7-1* displays a less severe phenotype (35% that of wild-type hypocotyl length) than do other BR dwarfs (e.g., 7% of wild type in *dwf4*; Choe et al., 1998). Furthermore, *dwf7-1* frequently displayed closed cotyledons and hooks similar to those of the wild type, whereas severe dwarfs, including *bri1/dwf2*, *cpd/dwf3*, and *dwf4*, showed expanded cotyledons and open hooks (data not shown).

Unlike severe dwarfs, such as *dwf4* and *cpd*, *dwf7-1* mutants are not mechanically sterile (Figure 2B). However, the average number of seeds in a silique is reduced in *dwf7-1* ($n = 12$) compared with that of the wild type for reasons yet to be identified ($n = 49$) (Table 1). Scanning electron microscopy

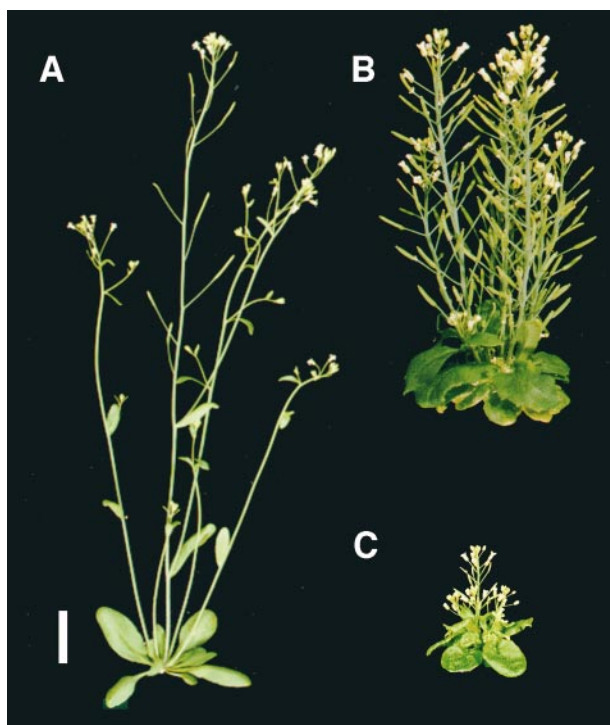


Figure 2. Morphology of Wild-Type and *dwarf7-1* Plants.

(A) Wild-type plant at 1 month of age. (B) and (C) *dwarf7-1* plants at 7 and 5 weeks of age, respectively. The characteristic dwarf phenotype, such as short robust stems, reduced fertility, and dark-green, round, and curled leaves, is shown in (B) and (C). At 7 weeks of age (B), wild-type plants had ceased growing, whereas *dwarf7-1* plants continued to grow. Bar = 2 cm.

(Figures 3A to 3C) demonstrates a relationship between fertility and floral structure. In the wild type (Figure 3A), the length of stamens is greater than or similar to that of the gynoecium (quantified in Figure 3D), facilitating dehiscence of pollen on the stigmatic surface. Although *dwarf7-1* flowers (Figures 3B and 3D) possess stamens and gynoecia that are shorter than those in the wild type, the fertility of *dwarf7-1* flowers is possible through a concomitant reduction in the length of both organs. In contrast, only stamen elongation is affected more severely in *dwarf4* flowers (Figures 3C and 3D). The short stamen length in *dwarf4* is likely to cause dehiscence of pollen on the ovary wall rather than on the stigmatic surface. In fact, when *dwarf4* pollen is transferred to either wild-type or *dwarf7-1* stigmas, viable seeds are made.

The common denominator for the various phenotypes found in *dwarf7-1* mutants is a reduction in longitudinal growth, which could be due to either a reduced number of cells or a failure in cell elongation. Observations made with other BR dwarf mutants suggest that the number of cells is comparable in the wild type and mutants (Kauschmann et

al., 1996; Nomura et al., 1997; Azpiroz et al., 1998). Figure 4 displays cell size in the wild type (Figure 4A) and *dwarf7-1* (Figure 4B) mutants. The length of cells in the epidermis, cortex, and xylem of *dwarf7-1* is greatly reduced (<30% of wild type). This reduced cell size is converted to the length of the wild type in response to application of BL (Figure 4C). Thus, the reduced organ length in *dwarf7-1* also is due to a failure of cell elongation.

We also have examined the organization of vascular bundles in wild-type and *dwarf7-1* mutants. Wild-type inflorescences possess eight vascular bundles (Figure 4D). However, the number of vascular bundles was reduced to six in *dwarf7-1* (Figure 4E). Furthermore, the spacing between the vascular bundles in *dwarf7-1* is irregular. In the wild type, interfascicular parenchyma cells alternate regularly with vascular bundles; however, cross-sections of *dwarf7-1* show that two vascular bundles are joined without being separated by parenchyma cells. Within a single vascular bundle, the size and number of xylem cells in *dwarf7-1* plants generally are reduced, whereas the number of phloem cells is similar to or even greater than that in the wild type. This characteristic abnormality of vascular bundle organization has been observed consistently in other BR dwarfs (Szekeres et al., 1996; S. Choe, C.P. Tissier, and K.A. Feldmann, unpublished data).

Biochemical Complementation of *dwarf7-1* with BL

Figure 5 demonstrates that *dwarf7-1* seedlings grown in BL-supplemented liquid media were remarkably sensitive to BL.

Table 1. Morphometric Analysis of Wild-Type and *dwarf7-1* Plants at 5 Weeks of Age

Measurement (<i>n</i> = 15)	Wild Type	<i>dwarf7-1</i>
Inflorescence		
Height (cm)	31.6 ± 0.9	4.5 ± 0.4
Number of inflorescences	3.9 ± 0.6	4.3 ± 0.5
Reproductive organs		
Number of reproductive organs	130.2 ± 12.9	89.3 ± 20.9
Length of siliques (mm)	14.8 ± 1.2	3.9 ± 0.8
Number of seeds ^a	49.7 ± 5.1	12.4 ± 2.4
Leaf		
Number of rosette leaves	9.1 ± 1.2	10.3 ± 1.9
Leaf blade width (cm) ^b	1.4 ± 0.1	1.4 ± 0.3
Leaf blade length (cm) ^b	3.0 ± 0.3	1.8 ± 0.3
Weight		
Fresh weight (g)	1.50 ± 0.19	0.51 ± 0.10
Dry weight (mg)	215 ± 29	53 ± 11
Fresh weight/dry weight	7.0 ± 0.3	9.7 ± 0.6

^aThe number of seeds per silique was determined after plant senescence.

^bThe second pair of rosette leaves.

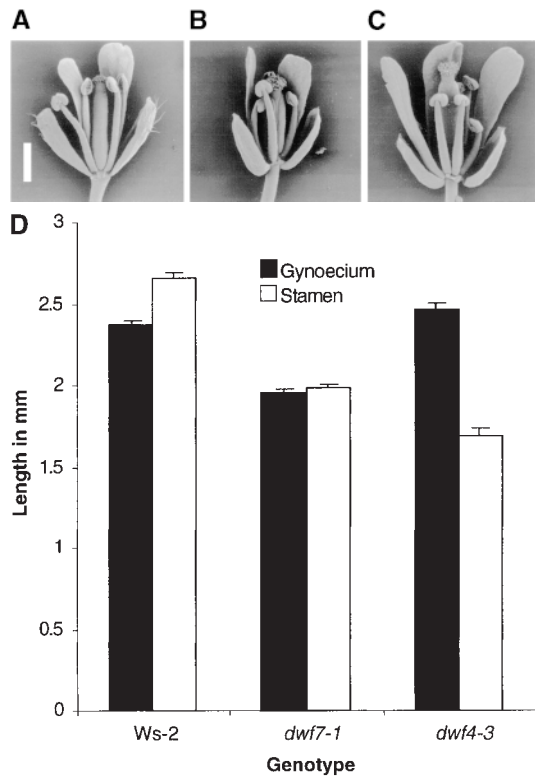


Figure 3. Analyses of Wild-Type, *dwf7-1*, and *dwf4-3* Flowers.

(A) to (C) Scanning electron microscopy of flowers from wild-type (ecotype Wassilewskija-2 [Ws-2]), *dwf7-1*, and *dwf4-3* plants. Flowers were harvested immediately after petal opening. The wild-type flower shown in (A) has a stamen length similar to or slightly greater than that of the gynoecium, facilitating pollen dehiscence on the stigmatic surface. A fertile *dwf7-1* flower is shown in (B) with a concomitant reduction in the size of the gynoecium and the stamen. A sterile *dwf4-3* flower is shown in (C) with shorter filaments than the gynoecium, preventing pollen dehiscence on the stigmatic surface. Bar in (A) = 1 mm.

(D) Measurements of gynoecia and stamens shown in (A) to (C). *dwf7-1* displays a concomitant reduction in the length of gynoecia and stamens, whereas *dwf4-3* displays a greater reduction in stamen length. Each data point represents the average length for five flowers. Standard errors are shown at each data point.

Growth in 1 nM BL induced significant elongation of *dwf7-1* hypocotyls (160% increase), whereas the wild-type increase was marginal (5%). Treatment with 10 and 100 nM BL completely rescued *dwf7-1* hypocotyls to wild-type length. The strongest response of the wild type to BL was obtained at 100 nM (Figure 5). Higher concentrations of BL (1 μ M) caused a stressed morphology, including inhibition of root growth and swollen, twisted, and fragile hypocotyls in both *dwf7-1* and wild-type plants (data not shown). After BL treatment of *dwf7-1*, cells in the treated region of the stem are similar in length to wild-type cells (Figure 4C).

Identification of the BR Biosynthetic Defect in *dwf7-1*

Biochemical complementation of *dwf7-1* following application of BL suggested that *dwf7-1* is likely to be defective in BR biosynthesis. To pinpoint the defective step in the BR biosynthetic pathway, *dwf7-1* mutants were treated with BR biosynthetic intermediates. Due to undetectable bioactivity of some early intermediates (CR to 6-oxocampestanol) in bioassays (Fujioka et al., 1995; Choe et al., 1998), these were not used. Instead, we chose three biologically active compounds, 22-OHCR, 6-deoxoCT, and BL, for these feeding tests (see Figure 1). Because the 22 α -hydroxylation reaction is reported to be mediated by DWF4 (Choe et al., 1998), biochemical complementation of *dwf* mutants other than *dwf4* by 22-OHCR places the defective step upstream of CR.

Figure 6A shows the response when inflorescences were treated daily for 1 week with these BR intermediates. ComPLEMENTING compounds induced growth of internodes and strongly increased pedicel length. *dwf7-1* pedicels treated with 22-OHCR and BL showed growth greater than or equal

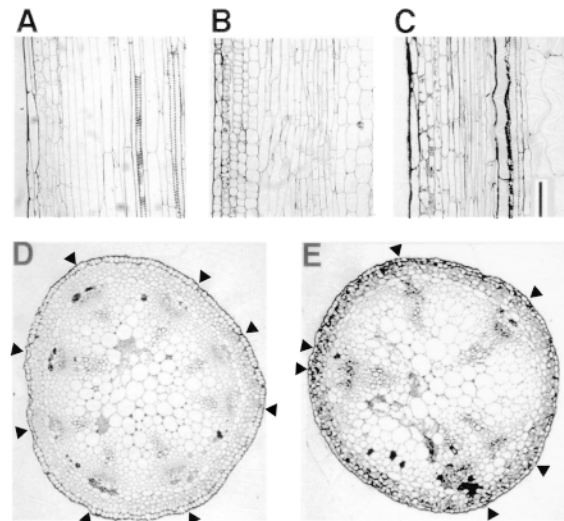


Figure 4. Light Microscopy of Wild-Type and *dwf7-1* Stems Sectioned Longitudinally and Transversally.

(A) Wild type.

(B) *dwf7-1*. Cell size is reduced drastically in many different tissues, such as the epidermis, cortex, and vasculature.

(C) *dwf7-1* plants treated with BL. Cells were restored to their wild-type length in response to daily application of 10^{-7} M BL for 1 week.

(D) and (E) Cross-sections of wild-type and *dwf7-1* stems, respectively. Positions of the vascular bundles are marked with triangles. Eight evenly spaced bundles are found in the wild type, whereas fewer and irregularly located bundles were present in *dwf7-1*.

Bar in (C) = 100 μ m for (A) to (C) (longitudinal sections); magnification $\times 100$ for (D) and (E).

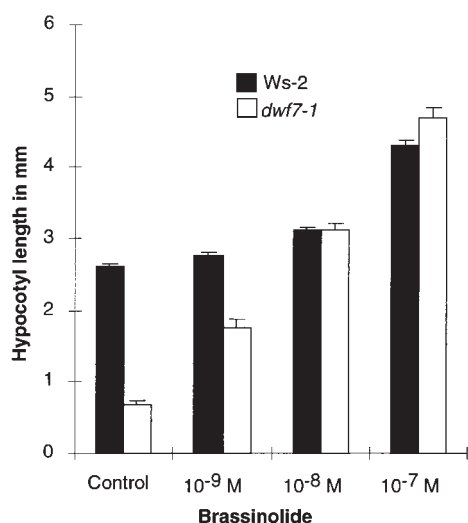


Figure 5. Response of Light-Grown Wild-Type and *dwf7-1* Hypocotyls to Different Concentrations of BL.

dwf7-1 responds to 10^{-9} M BL and is completely rescued by 10^{-8} M BL. Error bars indicate \pm SE.

to that of the wild type. Measurements of pedicel length shown in Figure 6B demonstrated that the three compounds tested, 22-OHCR, 6-deoxoCT, and BL, all increased *dwf7-1* pedicel length $>200\%$ as compared with the control, suggesting that the defective step in BR biosynthesis is located at or before the CR biosynthetic step. Similarly, 3-week-old inflorescences of *dwf7-2* were tested with 22-OHCR, 6-deoxoCT, teasterone, and BL. All four compounds induced significant elongation of pedicels and internodes (data not shown), indicating that *dwf7-1* and *dwf7-2* share the same biosynthetic defect.

As shown in Table 2, more definitive results indicating a specific defect in BR biosynthesis have been obtained from gas chromatography-selective ion monitoring (GC-SIM) analysis of endogenous BRs and sterols in *dwf7-1* plants. The endogenous levels of sterols, such as 24-MC, CR, and campestanol (CN), in wild-type plants, were 3800, 32,900, and 1140 ng/g fresh weight, respectively. However, the levels of all three sterols in *dwf7-1* mutants were extremely diminished at 3.1, 1.1, and 1.4% of the wild type, respectively, suggesting that the biosynthetic block is located before 24-MC. These data are consistent with the results of intermediate feeding studies (Figure 6).

Further biochemical feeding studies with ^{13}C -labeled mevalonic acid (MVA) and compactin, a MVA biosynthetic inhibitor, were performed to identify the specific sterol biosynthetic step defective in *dwf7-1* plants. In a preliminary experiment, the effects of compactin and MVA on the growth of Arabidopsis seedlings in liquid media were investigated. The growth of wild-type Arabidopsis seedlings was almost com-

pletely inhibited in the presence of 10 μM compactin. The inhibition, however, was restored to the level of controls by the simultaneous application of 4.5 mM of MVA (data not shown). Therefore, 4.5 mM ^{13}C -MVA and 10 μM compactin were added to Arabidopsis seedling cultures in the metabolic feeding studies. After 11 days in culture, sterols were extracted and purified by silica and octadecylsilane (ODS) cartridge columns and ODS-HPLC. Purified samples were derivatized and analyzed by gas chromatography-mass

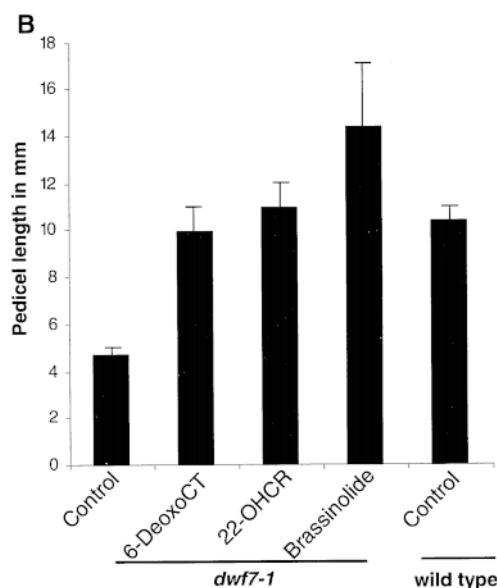


Figure 6. Wild-Type and *dwf7-1* Inflorescences Treated with BR Intermediates.

(A) From left to right, *dwf7-1* inflorescences treated with water, 22-OHCR, BL, and a wild-type inflorescence treated with water, respectively.

(B) Quantification of the inflorescence feeding test shown in (A). The lengths of pedicels treated with water, 6-deoxoCT, 22-OHCR, and BL were measured to the nearest millimeter ($n > 15$). The pedicels elongated greater than twofold in response to all the BRs tested, suggesting that the biosynthetic defect in *dwf7-1* resides before the production of CR. Error bars indicate \pm SE.

Table 2. Quantification of Endogenous BRs from Wild Type and *dwf7-1* by Using GC-SIM

BRs	Wild Type ^a	<i>dwf7-1</i> ^a
24-MC	3,800	118
CR	32,900	379
CN	1,140	16
6-Deoxoteasterone	0.05	NA ^b
6-Deoxytyphasterol	2.3	NA
6-Deoxocastasterone	4.0	ND ^c
Typhasterol	0.27	ND
CS	0.28	0.13
BL	0.2	ND

^aThe unit of measurement is nanograms per gram fresh weight.

^bNA, not analyzed.

^cND, not detected. The endogenous amount of the BR is less than the detection limit (~0.05 ng/g fresh weight).

spectrometry (GC-MS). As shown in Figure 7, ^{13}C -MVA was converted to $^{13}\text{C}_5$ -episterol and subsequent sterols, such as $^{13}\text{C}_5$ -24-MC and $^{13}\text{C}_5$ -CR in the wild type. However, the $^{13}\text{C}_5$ -5-dehydroepisterol and downstream compounds were not detected in *dwf7-1* mutants, whereas the precursor $^{13}\text{C}_5$ -episterol accumulated fourfold as compared with the wild type. In addition, an uncommon sterol, $^{13}\text{C}_5$ -7-dehydrocampestanol (24-epifungisterol), greatly accumulated (Figure 7). Two lines of evidence—a failure to convert episterol to subsequent sterols, such as 24-MC and CR, and accumulation of 7-dehydrocampestanol in *dwf7-1*—suggest that the defective step in *dwf7-1* is the C-5 desaturation step.

Molecular Characterization of *dwf7*

An EMS-induced mutant (*ste1-1*) of STE1 encoding a Δ^7 sterol C-5 desaturase did not possess a dwarf phenotype (Gachotte et al., 1995). However, because it is likely that *ste1-1* is a leaky allele, we hypothesized that *dwf7-1* might be a strong or null allele. We first sequenced the genomic DNA of the *STE1* gene and identified two introns and three exons by comparing them with the published *STE1* cDNA sequence. The organization of the *STE1* gene is represented schematically in Figure 8. Sequencing the *STE1* locus in the *dwf7* alleles revealed mutations. The mutations found in *dwf7-1* and *dwf7-2* were located in the third and the first exons, respectively. Both of the *dwf7* alleles contained a base change from a guanine to an adenine, converting tryptophan (TGG) to a stop codon (TAG in *dwf7-1* and TGA in *dwf7-2*).

In addition to creating a stop codon, the mutation in *dwf7-1* eliminated a *Hae*III restriction enzyme recognition site (GGCC to AGCC). Taking advantage of this restriction enzyme site change, we tested the linkage of this mutation to the *dwf7-1* phenotype. DNAs isolated from 17 different dwarf plants from a segregating F_2 population were sub-

jected to polymerase chain reaction (PCR) analysis by using S5D_3F and S5D_1R primers (underlines were used to distinguish forward or reverse primers from the gene acronym S5D), and the PCR products were digested with *Hae*III. Agarose gel electrophoresis definitively showed that none of the PCR products from 17 mutant templates was restricted, whereas products from wild-type templates were all restricted at the *Hae*III site (data not shown). These data suggest that the creation of the premature stop codon in exon 3 is the cause of the *dwf7-1*-conferred phenotype.

To better understand the importance of these nonsense mutations, we analyzed the sequence of STE1 in relation to other C-5 desaturase proteins isolated from fungi. The STE1 protein is composed of 281 predicted amino acids with a theoretical pI of 6.39 and molecular mass of 33 kD. Whereas yeast ERG3 (38% identical; Arthington et al., 1991; GenBank accession number M62623) is predicted to contain four transmembrane domains, STE1 possesses three putative transmembrane domains. The overall amino acid sequence identities of STE1 with C-5 desaturases from fission yeast (GenBank accession number AB004539) and *Candida glabrata* (Geber et al., 1995; GenBank accession number L40390) were 37 and 33%, respectively (gap creation weight of 4; gap extension weight of 1). In addition, multiple sequence alignment of STE1 with the three yeast sequences, shown in Figure 9, revealed that the transmembrane domains and histidine clusters, which were first reported by Gachotte et al. (1996), are well conserved between the proteins. The three characteristic histidine boxes flank the last transmembrane domain. The nonsense mutations are located in the first exon (*dwf7-2*) and the third exon, immediately before the third histidine box (*dwf7-1*), indicating that at least one histidine domain is deleted in each of the *dwf7* mutants as a result of the premature stop codons.

DISCUSSION

In this report, we present morphological, biochemical, and molecular analysis of *Arabidopsis dwf7* mutants. Morphologically, *dwf7-1* plants display a dramatic reduction in the length of many different organs examined, and this size reduction is attributable to a defect in cell elongation. Biochemically, *dwf7-1* hypocotyls were converted completely to wild-type length with the application of BL, suggesting a deficiency in BRs. In agreement with this, BR intermediate feeding analysis, accompanied by analysis of endogenous levels of BRs and sterols by using GC-SIM, indicated that *dwf7-1* is defective specifically in the Δ^7 sterol C-5 desaturase step of the sterol biosynthetic pathway. Sequencing of the Δ^7 sterol C-5 desaturase gene in *dwf7-1* and *dwf7-2* revealed premature stop codons, suggesting loss-of-function mutations. Thus, we propose that a shortage of sterols leads to a drastic reduction of BR levels in *dwf7-1* and *dwf7-2* and to the characteristic dwarf phenotype.

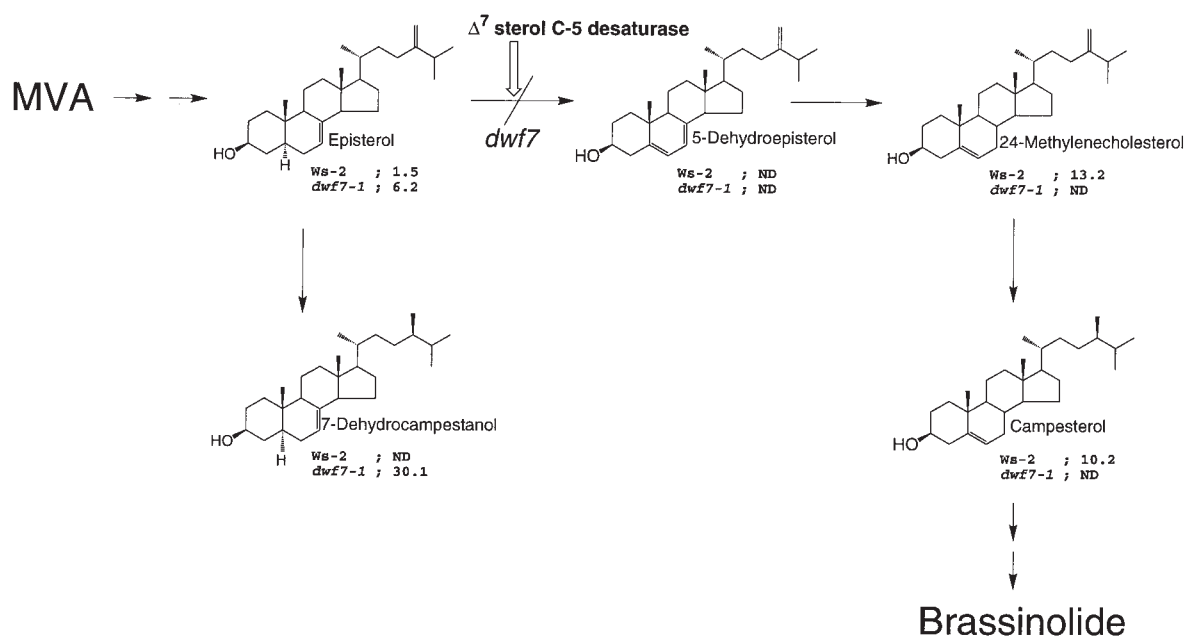


Figure 7. GC-MS Analysis of Wild-Type and *dwf7-1* Seedlings Fed with ^{13}C -MVA in the Presence of Compactin, an Inhibitor of MVA Biosynthesis. Accumulation of episterol with a simultaneous decrease of downstream intermediates, including 24-MC and CR, predicts that the C-5 desaturation step is blocked in *dwf7-1* plants. The units are in micrograms per 5 g fresh weight of tissue. The designation ND (not detected) means that the quantity is lower than the detection limit. Ws-2, Wassilewskija-2 wild type.

BRs Regulate Cell Elongation and Cell Differentiation

The overall morphology of plants is dependent on three factors: cell size, shape, and number (Cosgrove, 1997). Various signals modulate these factors. Environmental signals, such as water, temperature, and light, are transduced to invoke internal hormone signals, including auxins, gibberellins, and BRs. These signals then trigger the cell elongation process, including but not limited to cell wall loosening by xyloglucan endotransglycosylases and expansins. Thus, a block in any of the signal transduction cascades from the environmental signals to the cell elongation process could result in dwarfism. Mutants resistant to or deficient in classic hormones, such as auxin (e.g., *auxin resistant2* [*axr2*]; Timpte et al., 1992) and gibberellin ([*ga1* to *ga5* and *gai*]; Koornneef and van der Veen, 1980; Koornneef et al., 1985), often result in dwarfism. Thus, we first tested whether *dwf7* is either rescued by or resistant to exogenous application of these hormones. Three-week-old *dwf7-1* plants sprayed with 0.1 mM GA_3 responded, as did the wild type (<10% increase of inflorescence height; data not shown); however, GA_3 did not rescue the *dwf7-1* phenotype. In addition, *dwf7-1* roots grown on indole acetic acid-supplemented agar media (0.1 μM) displayed stunted morphology similar to that of the wild type, suggesting that *dwf7-1* is not resistant to the exogenous application of auxin (data not shown). The reduction of

hypocotyl length in *dwf7-1* was rescued by the application of BL (Figure 5). Both wild-type and *dwf7-1* plants responded to BL, but *dwf7-1* plants were hypersensitive. The length of *dwf7-1* hypocotyls was increased 160% in response to 1 nM BL as compared with the untreated control, whereas the wild type responded marginally (5%). In addition, application of BRs to 3-week-old *dwf7-1* plants induced the growth of many different organs, including stems, leaves, siliques, petioles, and pedicels, suggesting that the major defect in *dwf7-1* is a deficiency of BL.

Apart from a reduction in cell elongation, a deficiency of endogenous BRs resulted in altered organization of vascular tissue in the inflorescence (Figure 4E). Szekeres et al. (1996) showed that the number of xylem cells in *cpd* was decreased as compared with the wild type, whereas the number of phloem cells was increased. The authors reasoned that this could be due to unequal division of cambial cells. Furthermore, previous studies on the effects of BRs on vascular development indicated that BRs play a role in tracheary element formation (Clouse and Zurek, 1991; Iwasaki and Shibaoka, 1991). Because BRs also have been found in the cambial region of pine, indicative of an important role in this tissue (Kim et al., 1990), we hypothesize that the deficiency of BRs in dwarf mutants caused changes in cell fate in vascular cambial cells through yet unknown mechanisms.

Auxins also are known to be a major factor affecting differentiation of the vascular system (Aloni, 1987). Lincoln et al. (1990) showed that stem cross-sections of *axr1* displayed altered development of the vascular system. The vascular bundles in *axr1* mutants are located peripherally and are not as regularly spaced as compared with those in wild-type plants (Lincoln et al., 1990). Furthermore, as opposed to the reduced number of vascular bundles in *dwf7-1* (five to seven), *axr1* plants possess a greater number of bundles (eight to nine) as compared with the wild type (six to eight). Thus, it seems that auxins and BRs play opposing roles in determining the number of vascular bundles. Two other assays in which auxin and BR interactions have been demonstrated are the rice lamina bending assay and hypocotyl hook opening bioassay. Results from these assays include the fact that the degree of effect caused by the combined application of auxin and BR was greater than was the sum of the effect of each, indicative of a synergistic effect of the two hormones (Yopp et al., 1981; Takeno and Pharis, 1982; reviewed in Mandava, 1988). However, the details of the mechanisms for interactive and independent action remain to be elucidated.

It needs to be pointed out that hypocotyl growth in darkness is accomplished through both GA- and BR-dependent cell elongation processes. One piece of evidence for dependence on both GA and BR is that *dwf7-1* hypocotyls elongated fivefold in response to darkness as compared with light-grown hypocotyls (data not shown), although they are still shorter than those of the wild type. Because BL levels are not detectable in *dwf7-1* plants (Table 2), growth of *dwf7-1* in the dark could be accomplished mostly by GA-dependent cell elongation processes. Peng and Harberd (1997) and Azpiroz et al. (1998) found that both *gai* and *dwf4*, respectively, partially suppressed the stem elongation phe-

notype of a light receptor mutant, *hy*, suggesting that hypocotyl elongation in the absence of light inhibition requires independent growth contributed by both GA and BRs.

dwf7 Plants Are Defective in Sterol Biosynthesis Leading to BRs

A defect either in a biosynthetic enzyme or a factor modulating an enzymatic activity could lead to deficiency of endogenous BRs. To place *dwf7* at a specific step in the proposed BR biosynthetic pathway, we first chose to perform feeding studies with BR biosynthetic intermediates. Rescue of *dwf7-1* by exogenous application of 22-OHCR suggests that the biosynthetic defect likely resides before the production of CR (Figure 6A). Consistent with the results from feeding studies, the endogenous levels of 24-MC, CR, and CN were extremely reduced in *dwf7-1* (Table 2). These data indicate that the biosynthetic defect is before 24-MC; *dwf7-1* contains only 3% of 24-MC as compared with the wild type. When the phenotypes of *dwf7-1* are compared with the downstream biosynthetic mutant *dwf4* and the BR-insensitive *bri1* (*dwf2*) mutant (Clouse et al., 1996; S. Choe and K.A. Feldmann, unpublished data), it is obvious that *dwf7-1* displays a weaker phenotype despite being a presumptive null mutation. This suggests that there could be an alternative sterol and BR biosynthetic pathway or that there are duplicate genes at individual steps. Providing evidence for the duplicate gene hypothesis, we recently cloned a homolog of the *DWF7/STE1* gene (named *HOMOLOG OF DWF7, HDF7*). *HDF7* is 80% identical in amino acid sequence with *STE1* (A. Tanaka, S. Choe, and K.A. Feldmann, unpublished data). Similarly, Fujioka et al. (1997) reported that the endogenous level of CN in *det2*, which is defective in a step between CR

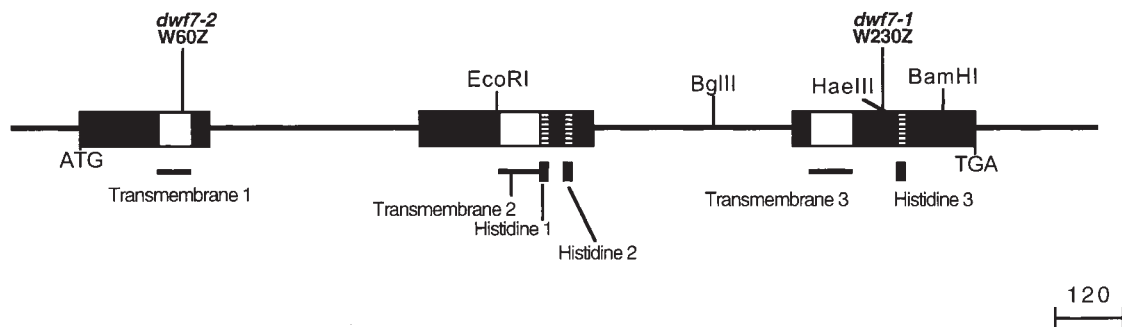


Figure 8. Schematic Representation of the *STE1* Gene.

Comparison of cDNA and genomic DNA sequences revealed three exons (thick boxes) and two introns (horizontal bars). The single open reading frame encodes a protein of 281 amino acids. The *dwf7-2* (*ste1-3*) mutation is located in the first exon, changing a tryptophan to a stop codon. The *dwf7-1* (*ste1-2*) mutation also changes a tryptophan to a stop codon (amino acid position 230). The three white boxes indicate the transmembrane domains, and the three histidine boxes are lightly shadowed. The figure is drawn to scale by using the GCK software (Textco, Inc., West Lebanon, NH). Bar = 120 bp.

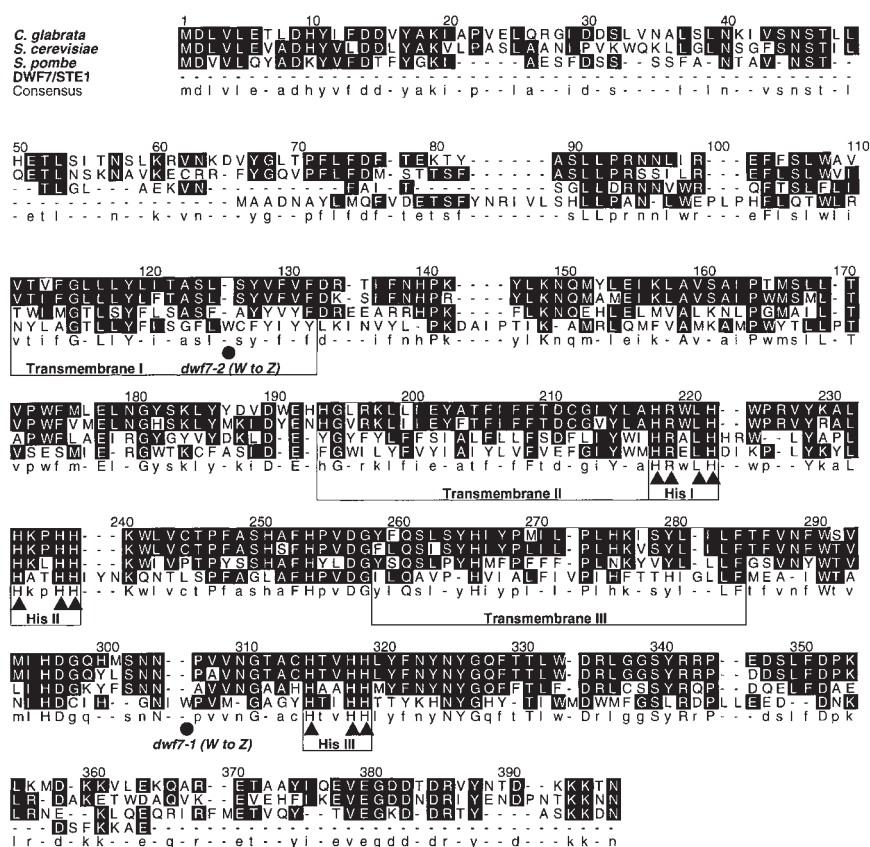


Figure 9. Multiple Sequence Alignment of DWF7/STE1 with Known Sequences for Δ^7 Sterol C-5 Desaturases.

GenBank accession numbers for the sequences are M62623 (*S. cerevisiae*), AB004539 (*Schizosaccharomyces pombe*), L40390 (*C. glabrata*), and AF105034 (DWF7/STE1, *Arabidopsis*). The conserved transmembrane domains and histidine clusters are boxed and labeled. The positions of the premature stop codons in *dwf7-1* and *dwf7-2* are indicated with filled circles. Histidine residues in each conserved histidine box are identified with filled triangles. Capital letters stand for residues conserved among all sequences, whereas lowercase letters mean $\geq 50\%$ identical. Dashes indicate gaps introduced to maximize alignment. Multiple sequence alignment was performed using PILEUP in the Genetics Computer Group software (Madison, WI) with a gap creation penalty of 4 and a gap extension parameter of 1. The annotation of the aligned sequences was performed using the ALSCRIPT software (Barton, 1993).

and CN, is $\sim 10\%$ that of the wild-type amount. The authors hypothesized that the 10% leakage through the defective step in *det2* mutants, even in a null allele, could be associated with a second copy of *DET2* that lightly hybridizes in DNA gel blot analyses.

Placing *dwf7* at a single sterol biosynthetic step was accomplished through feeding studies with ^{13}C -MVA and compactin. A greater than fourfold accumulation of episterol accompanying the absence of downstream intermediates in *dwf7-1* indicates that the Δ^7 sterol C-5 desaturase step is blocked in *dwf7*. In addition, the feeding studies identified an accumulation of 7-dehydrocampestanol, which is an uncommon sterol in plants (Figure 7). Accumulation of this compound only in *dwf7-1* suggests that sterol biosynthesis in *dwf7-1* could proceed to a C-24 reduction step, skipping C-5

desaturation as well as the next immediate C-7 reduction. The C-24 reductase seems to convert episterol independently of the immediate upstream enzyme. The absence of a detectable amount of C-7-reduced compounds in *dwf7-1* suggests that the enzymatic step is highly dependent on the C-5 desaturation reaction. This confirms the sequence of reactions originally proposed by Taton and Rahier (1991, 1996).

***dwf7* Mutants Produce Nonfunctional Δ^7 Sterol C-5 Desaturase Due to Premature Stop Codons**

The Δ^7 sterol C-5 desaturase-mediated reaction is common to both photosynthetic and nonphotosynthetic organisms. Many genes encoding a C-5 desaturase have been cloned

from fungi. First, Arthington et al. (1991) cloned the *ERG3* gene from *Saccharomyces cerevisiae*. The authors found that viable *erg3* mutants, which normally accumulate Δ^7 sterols, were restored to wild-type phenotype when transformed with a wild-type genomic clone of the Δ^7 sterol C-5 desaturase gene. Taguchi et al. (1994) showed that the yeast mutant *syr1* displays dual phenotypes, resistance to the phytotoxin syringomycin and susceptibility to higher concentrations of Ca^{2+} , presumably due to altered membranes. Sequencing the *ERG3* locus in the *syr1* mutant revealed that *syr1* is an allele of *ERG3*. Furthermore, Geber et al. (1995) cloned both *ERG3* and *ERG11* (14 α -sterol-demethylase) from *C. glabrata*. The authors found that lethal *erg11* mutations can be suppressed by an additional mutation in *erg3*. They reasoned that formation of toxic 3 β ,6 α -diol sterols in *erg11* mutants is prevented due to the defect in C-5 desaturation in *erg11 erg3* double mutants.

In plants, Gachotte et al. (1995) found that the *Arabidopsis ste1-1* mutant, which is deficient in C-5 desaturated sterols, can be partially complemented by the yeast *ERG3* gene. Accordingly, the authors hypothesized that *ste1-1* possesses a mutation in the sterol C-5 desaturase gene. They isolated the *Arabidopsis* C-5 desaturase gene through heterologous complementation of a yeast *erg3* null mutant with an *Arabidopsis* cDNA library (Gachotte et al., 1996). Finally, the partial human cDNA for the C-5 desaturase has been identified by Matsushima et al. (1996). Alignment of the sequences of these enzymes revealed that C-5 desaturases from different organisms are highly conserved in overall sequence as well as in specific domains. The overall amino acid sequence identity and similarity among STE1 and ERG3 and the human ortholog is 38% (50%) and 35% (47%), respectively (similarity within parentheses). As indicated in Figures 8 and 9, key domains including the transmembrane domains and the histidine clusters are well conserved between all the C-5 desaturases.

Closely spaced histidine residues, HX₃H in α helices, serve as typical metal binding motifs in many proteins (Regan, 1993). Shanklin et al. (1994) showed that three membrane-associated bacterial enzymes, fatty acid desaturase, alkane hydroxylase, and xylene monooxygenase, possess eight histidine residues that are conserved in three regions dispersed in these enzymes, HX₍₃₋₄₎H, HX₍₂₋₃₎HH, and HX₍₂₋₃₎HH (where X stands for any amino acid). DNA constructs containing site-directed mutations at any of these eight histidine residues of the rat Δ^9 desaturase failed to complement the yeast mutant *ole1*, which is defective in the same enzymatic step, suggesting that the individual histidine residues are essential for the function of the enzyme. On the basis of these observations, Shanklin et al. (1994) hypothesized that the histidine clusters conserved in these enzymes constitute new structural domains of diiron binding centers (Shanklin et al., 1994). Gachotte et al. (1996) first recognized the conserved histidine clusters in STE1 and yeast proteins. We confirmed that the motifs are highly conserved in STE1 and the yeast ERG3 enzymes with the same

context of HX₃H, HX₂HH, and HX₂HH (Figure 9), revealing the presence of a putative iron binding motif in Δ^7 sterol C-5 desaturases.

More direct evidence of metal ion involvement in Δ^7 sterol C-5 desaturase function was obtained by Taton and Rahier (1996). These authors discovered that the enzyme prepared from maize microsomes is inhibited by cyanide, whereas it is insensitive to carbon monoxide, indicative of the involvement of a metal ion, presumably an iron, for the proper function of the enzyme. Furthermore, we noticed that the typical histidine moiety also was conserved in a different group of oxidases such as RANP-1 (Uwabe et al., 1997), C-4 methyl sterol oxidase (Li and Kaplan, 1996), and aldehyde decarboxylase (Aarts et al., 1995). Occurrence of these histidine boxes in a wide variety of oxidases indicates that this domain plays a common and essential role in the function of membrane oxidases. Therefore, it is likely that the mutations in *dwf7-1* and *dwf7-2* would be deleterious to protein function. The premature stop codon in *dwf7-2* would eliminate all important known domains, whereas the third histidine box and several amino acid residues that are 100% conserved in the C terminus of the protein are eliminated in *dwf7-1*. Intriguingly, the location of the mutations in *dwf7-1* and *dwf7-2* seems to be related to the phenotypic severity of the mutant alleles. *dwf7-2*, which contains an earlier stop codon, was shorter in height and less fertile than *dwf7-1*. A more precise comparison between the two alleles is not possible because the EMS allele, *dwf7-2*, has not been outcrossed to remove any background mutations that might have increased the severity of the phenotype of *dwf7-2*. Despite the differences in severity, both *dwf7* alleles would be predicted to be complete loss-of-function alleles. The resulting nonfunctional enzyme would cause a block in sterol biosynthesis. This shortage of substrate sterols in *dwf7-1* and *dwf7-2* would lead to a deficiency of endogenous BRs and cause the characteristic dwarfism in *dwf7* plants.

METHODS

Plant Growth

For sterile growth of *Arabidopsis thaliana* plants, seeds of mutants and the wild type were sterilized (50% Clorox and 0.005% Triton X-100) for 8 min, washed three times with sterile distilled water, and dried with 95% ethanol. The seeds were sprinkled on 0.8% agar-solidified media or in liquid media containing 1 \times Murashige and Skoog (1962) salts and 0.5% sucrose (pH 5.8 with KOH). For the plants grown in the dark, the seeds on the plates were illuminated for 3 hr (240 $\mu\text{mol m}^{-2} \text{sec}^{-1}$) before being wrapped with two or three layers of aluminum foil. For the mature plants used for morphometric analysis and gas chromatography-selective ion monitoring (GC-SIM) studies, seeds were planted on soil (Metromix 350; Grace Sierra Co., Milpitas, CA) presoaked with distilled water. The flats containing the pots were covered with plastic wrap and cold-treated at 4°C for 2 days before transfer to a growth chamber (16 hr of light [240 $\mu\text{mol m}^{-2} \text{sec}^{-1}$] and 8 hr of dark

at 22 and 21°C, respectively, and 75 to 90% humidity). The plastic wrap was removed after 2 to 3 days. The pots were subirrigated in distilled water or Hoagland's nutrient solution as required.

Morphometric and Physiological Analysis

At 5 weeks of age, the various morphological traits listed in Table 1 were measured. The number of seeds per silique was determined after the plants were completely dried. Unopened siliques from each plant were selected and crushed, and the number of seeds was counted under a dissecting microscope. To measure the fresh and dry weight, we cut the aerial parts of the plants and immediately weighed them to obtain the fresh weight; the plants were then completely dried in a 60°C oven for 5 days before measuring the dry weight. Observations on the structure of flowers were made with flowers at stage 14 (Smyth et al., 1990), which are right beneath the cluster of developing flowers at the shoot apices. Individual organs of a flower were separated under the dissecting microscope. The length of the organs was measured to a tenth of a millimeter, and the four longest stamens for each flower were measured and the mean value calculated.

The anatomical studies using a scanning electronic microscope and a light microscope were performed as described by Azpiroz et al. (1998).

Mapping and Sequencing of the *DWARF7* Locus

The mapping of *dwarf7* (*dwf7*) was performed using simple sequence length polymorphism (SSLP) markers (Bell and Ecker, 1994). Briefly, *dwf7-1* mutants (Wassilewskija-2 [Ws-2] background) were crossed to Columbia wild-type plants. Genomic DNA was isolated (Dellaporta et al., 1983) from individual F₂ dwarf plants. To locate the mutation to one of the five chromosomes, 20 individual plants were tested with at least two SSLP markers per chromosome. The polymerase chain reaction (PCR) amplified products were analyzed on 4% agarose gels in 1 × TAE buffer (40 mM Tris-acetate and 10 mM EDTA). Once the *dwf7-1* mutation was shown to be linked to the *nga162* marker located on chromosome 3 (recombination ratio 11.9%), we tested marker *nga172*, which maps at 2.2 centimorgans. No recombination was detected between the *dwf7-1* mutation and *nga172* when 86 chromosomes were tested, suggesting that *dwf7-1* is linked closely to the *nga172* marker. Linkage between the markers and the dwarf phenotype was determined according to Koornneef and Stam (1992).

PCR products amplified using primer sets derived from the cDNA sequence of *STEROL1* (*STE1*) were subjected to sequencing. To design sets of primers that do not fall in exon-intron junctions, we predicted possible splice sites by using the RNASPL program available at the Internet site of Baylor College of Medicine (Houston, TX; <http://dot.imgen.bcm.tmc.edu:9331/seq-search/gene-search.html>). Primers were designed using the Primer Selection software of DNASTAR (DNASTAR Inc., Madison, WI). Oligonucleotide sequences 5' to 3' are CAGTGTGAGTAATTAGCATTACTA (S5D_FF), GGAAAGATCATCAAACATTTACATGT (S5D_LR), GCGCAATCTTCTTTGCTTT (S5D_1F), TGGACAACAACAACAAGA (S5D_1R), GATGCACAGAGAGCTTCATGAC (S5D_2F), CCGGCAATGGAGAGAGTGTAT (S5D_2R), CACCCATCATATCTACAACAA (S5D_3F), and CATCTTTGCCGCGCAATCTAT (S5D_4F) (underlines were added to distinguish forward or reverse primers from the gene acronym S5D). Primers were purchased from Genosys Biotechnologies, Inc. (The Woodlands, TX).

For template DNA, genomic DNA was isolated from two or three leaves of *dwf7-1* and wild-type plants according to the method described by Krysan et al. (1996). Amplification of the DNA fragment spanning the whole coding region was performed with the S5D_4F and S5D_1R primer set with Taq polymerase (Boehringer Mannheim).

Standard PCR reaction mixtures, 1 × PCR buffer (10 mM Tris-HCl, 1.5 mM MgCl₂, and 50 mM KCl, pH 8.3), 0.2 μM each of forward and reverse primer, 0.2 mM each deoxynucleotide triphosphates, 1 ng of genomic DNA, and 2 units of Taq polymerase were subjected to a PCR program consisting of an initial denaturation at 95°C for 2 min and then for 35 cycles (95°C for 30 sec, 56°C for 30 sec, and 72°C for 2.5 min), with a final elongation step of 7 min at 72°C. PCR-amplified DNA was size-separated on 0.8% agarose gels in 1 × TAE, and the resulting DNA bands were gel-purified using a DNA purification kit (Bio-Rad). The concentration of the extracted DNA was measured by comparing the band intensity with a DNA mass standard (Bethesda Research Laboratories). Sequencing of the DNA was performed at the Arizona Research Laboratory (University of Arizona, Tucson). DNA sequence analysis was conducted using software packages, including one from Genetics Computer Group (Madison, WI) and other database search tools available on the Internet.

The base change in *dwf7-1* eliminated the recognition site for a restriction enzyme *HaeIII* by converting the sequence from GGCC to AGCC. Thus, we utilized this polymorphism to test the cosegregation of the dwarf phenotype with the mutation. The 0.8 kb of DNA spanning the mutation was amplified using S5D_3F and S5D_1R primers from 17 different dwarf plants from the mapping lines. Two microliters from each 20 μL of PCR-amplified DNA was digested with the restriction enzyme *HaeIII* (Boehringer Mannheim). After complete digestion, the samples were resolved on a 2% agarose gel in 1 × TAE buffer.

Genomic DNA sequence flanking the cDNA was identified by sequencing the products obtained from thermal asymmetric interlaced PCR (TAIL PCR) (Liu et al., 1995). Two sets of primers were used to amplify the 5' and 3' flanking DNA. Oligonucleotide sequences 5' to 3' are GTAGAAGCACCAGAGGAAACCGGAGATGAAGT (D7-5-1; melting temperature of 69°C), AAGTATAGTAGGGTCCGGCCGAGGTA (D7-5-2; melting temperature of 64°C), ATAGATTCGCCGCAAAAGATGACTC (D7-5-3; melting temperature of 63°C), TGCAGGATACCATACGATACACCACACGACAT (D7-3-1; melting temperature of 68°C), CATACGATACACCACACGACATACAAGCATAACTA (D7-3-2; melting temperature of 67°C), and ATATGGATGATTGGATGTTGGCTCTC (D7-3-3; melting temperature of 63°C). The melting temperature of each primer was calculated with the formula $69.3 + 0.41 (\%GC) - 650/L$ (Mazars et al., 1991), where L is length of primer. Arbitrary degenerate primers AD1, AD2, and AD3 were synthesized according to the sequence described by Liu et al. (1995). TAIL PCR was performed according to the program originally described by Liu et al. (1995). TAIL PCR-amplified DNA was separated on 1% agarose gels and gel extracted for sequencing.

Feeding Experiments

Biochemical complementation of *dwf7-1* plants with different concentrations of brassinolide (BL) was performed in liquid media. BL-supplemented (control, 10⁻⁹, 10⁻⁸, and 10⁻⁷ M) sterile liquid media (1.5 mL) was dispensed into wells of a 24-well plate (Corning Co., Corning, NY). Three seedlings, germinated on agar-solidified media, were transferred into each well. After a week of growth with continuous shaking (230 rpm), the seedlings were lightly stained with toluidine blue, and hypocotyls and roots were measured to the nearest millimeter.

Feeding experiments using biosynthetic intermediates were performed with 3-week-old mutant plants. The intermediates tested were diluted to the desired concentration with water containing 0.01% Tween 20. Two microliters of each brassinosteroid (BR) solution was applied daily to the shoot tips of plants by using a micro pipette. After 1 week of treatment, total growth of inflorescence and pedicels was measured to the nearest millimeter ($n = 15$).

Analysis of Endogenous BRs

Plants were grown for 5 weeks on soil. Two hundred grams of the aerial parts of plants, including stems, flowers, leaves, and siliques, was harvested and subjected to BR extraction. The procedure for extraction and analysis of BR intermediates by using GC-SIM has been described (Fujioka et al., 1997).

^{13}C -Labeled Mevalonic Acid Feeding Experiments

Before feeding experiments, seedlings were germinated and grown on $0.5 \times$ Murashige and Skoog agar medium in the light at 22°C (25 mL per dish). Eight days after sowing, the seedlings were transferred to a 200-mL flask containing 30 mL of Murashige and Skoog media supplemented with 3% sucrose (Ws-2, five seedlings; *dwf7-1*, 40 seedlings).

Compactin (mevastatin; Sigma) was converted to its sodium salt as described previously (Kita et al., 1980). DL-Mevalonolactone-2- ^{13}C (^{13}C -MVA; Isotec, Miamisburg, OH) was dissolved in methanol. Solutions of compactin and ^{13}C -MVA were added aseptically to each 200-mL flask (final concentration, 10 μM compactin and 4.5 mM ^{13}C -MVA) just after the seedlings were transferred, and seedlings were allowed to grow for 11 days at 22°C in the light on a shaker (110 rpm). After incubation, the seedlings (~5 g fresh weight of both Ws-2 and *dwf7-1* plant materials) were extracted with methanol (250 mL), and the extract was partitioned between CHCl_3 and H_2O . The CHCl_3 -soluble fraction was purified with a silica cartridge column (Sep-Pak Vac 12 cc; Waters, Milford, MA), which was eluted with 20 mL of CHCl_3 . The eluate was purified with an octadecylsilane (ODS) cartridge column (Sep-Pak PLUS C18; Waters), which was eluted with 20 mL of methanol. The fraction was subjected to HPLC on an ODS column as follows: column, Senshu Pak ODS 4150-N (150 \times 10 mm); solvent, methanol; flow rate, 2 mL/min; and detection, UV 205 nm. Fractions were collected every 0.5 min (between retention times of 10 to 20 min). Main fractions of each sterol were as follows: 5-dehydroepisterol (retention time of 11.5 to 12 min), episterol (retention time of 12.5 to 13 min), 24-methylenecholesterol (24-MC; retention time of 13 to 13.5 min), 7-dehydrocampestanol (retention time of 14.5 to 15 min), and campesterol (CR; retention time of 15.5 to 16 min).

Each fraction was converted to a trimethylsilyl derivative and analyzed by gas chromatography-mass spectrometry (GC-MS). GC-MS analyses were performed on a JEOL Automass JMS-AM 150 mass spectrometer (Tokyo, Japan) connected to a Hewlett-Packard 5890A-II gas chromatograph with a capillary column DB-5 (0.25 mm \times 15 m; 0.25- μm film thickness). The analytical conditions were the same as previously described (Fujioka et al., 1997).

5-Dehydroepisterol, episterol, and 7-dehydrocampestanol were chemically synthesized (S. Takatsuto, C. Gotoh, T. Noguchi, and S. Fujioka, unpublished data).

ACKNOWLEDGMENTS

We thank Brian P. Dilkes, Alice Traut, and Xuelu Wang for their technical assistance. We thank Pierre Benveniste and his collaborators for sharing unpublished data on *ste7-1*. S.C. thanks the Korean government for support as an overseas scholar (Grant No. 93-0019). A.T. thanks the JAERI and Science and Technology Agency of Japan. We also thank the staffs of the sequencing and imaging facilities in the Arizona Research Laboratory at the University of Arizona (Tucson). S.F. acknowledges support from RIKEN (President's Special Research Grant) and from a grant-in-aid for scientific research (B) from the Ministry of Education, Science, Sports, and Culture of Japan (Grant No. 10460050). K.A.F. acknowledges support from the National Science Foundation (Grant No. 9604439).

Received November 11, 1998; accepted November 18, 1998.

REFERENCES

- Aarts, M.G.M., Keijzer, C.J., Stiekema, W.J., and Pereira, A. (1995). Molecular characterization of the *CER1* gene of Arabidopsis involved in epicuticular wax biosynthesis and pollen fertility. *Plant Cell* **7**, 2115–2127.
- Aloni, R. (1987). Differentiation of vascular tissue. *Annu. Rev. Plant Physiol.* **38**, 179–204.
- Arthington, B.A., Hoskins, J., Skatrud, P.L., and Bard, M. (1991). Nucleotide sequence of the gene encoding yeast C-8 sterol isomerase. *Gene* **107**, 173–174.
- Azpiroz, R., Wu, Y., LoCascio, J.C., and Feldmann, K.A. (1998). An Arabidopsis brassinosteroid-dependent mutant is blocked in cell elongation. *Plant Cell* **10**, 219–230.
- Bach, T.J., and Benveniste, P. (1997). Cloning of cDNAs or genes encoding enzymes of sterol biosynthesis from plants and other eukaryotes: Heterologous expression and complementation analysis of mutations for functional characterization. *Prog. Lipid Res.* **36**, 197–226.
- Bak, S., Kahn, R.A., Olsen, C.E., and Halkier, B.A. (1997). Cloning and expression in *Escherichia coli* of the obtusifoliosol 14- α -demethylase of *Sorghum bicolor* (L.) Moench, a cytochrome P450 orthologous to the sterol 14- α -demethylases (CYP51) from fungi and mammals. *Plant J.* **11**, 191–201.
- Barton, G.J. (1993). ALSCRIPT, a tool to format multiple sequence alignments. *Protein Eng.* **6**, 37–40.
- Bell, C.J., and Ecker, J.R. (1994). Assignment of 30 microsatellite loci to the linkage map of Arabidopsis. *Genomics* **19**, 137–144.
- Benveniste, P. (1986). Sterol biosynthesis. *Annu. Rev. Plant Physiol.* **37**, 275–308.
- Bouvier-Navé, P., Husselstein, T., Desprez, T., and Benveniste, P. (1997). Identification of cDNAs encoding sterol methyltransferases involved in the second methylation step of plant sterol biosynthesis. *Eur. J. Biochem.* **246**, 518–529.
- Choe, S., Dilkes, B.P., Fujioka, S., Takatsuto, S., Sakurai, A., and Feldmann, K.A. (1998). The *DWF4* gene of Arabidopsis encodes

- a cytochrome P450 that mediates multiple 22 α -hydroxylation steps in brassinosteroid biosynthesis. *Plant Cell* **10**, 231–243.
- Choi, Y.H., Fujioka, S., Nomura, T., Harada, A., Yokota, T., Takatsuto, S., and Sakurai, A.** (1997). An alternative brassinolide biosynthetic pathway via late C-6 oxidation. *Phytochemistry* **44**, 609–613.
- Clouse, S.D., and Zurek, D.** (1991). Molecular analysis of brassinolide action in plant growth and development. In *Brassinosteroids: Chemistry, Bioactivity and Applications*, H.G. Cutler, T. Yokota, and G. Adam, eds (Washington DC: American Chemical Society), pp. 122–140.
- Clouse, S.D., Langford, M., and McMorris, T.C.** (1996). A brassinosteroid-insensitive mutant in *Arabidopsis thaliana* exhibits multiple defects in growth and development. *Plant Physiol.* **111**, 671–678.
- Corey, E.J., Matsuda, S.P.T., and Bartel, B.** (1993). Isolation of an *Arabidopsis thaliana* gene encoding cycloartenol synthase by functional expression in a yeast mutant lacking lanosterol synthase by the use of a chromatographic screen. *Proc. Natl. Acad. Sci. USA* **90**, 11628–11632.
- Cosgrove, D.J.** (1997). Relaxation in a high-stress environment: The molecular bases of extensible cell walls and cell enlargement. *Plant Cell* **9**, 1031–1041.
- Dellaporta, S.L., Wood, J., and Hicks, J.B.** (1983). A plant DNA miniprep: Version II. *Plant Mol. Biol. Rep.* **1**, 19–21.
- Fujioka, S., and Sakurai, A.** (1997). Brassinosteroids. *Nat. Prod. Rep.* **14**, 1–10.
- Fujioka, S., Inoue, T., Takatsuto, S., Yanagisawa, T., Yokota, T., and Sakurai, A.** (1995). Biological activities of biosynthetically related congeners of brassinolide. *Biosci. Biotechnol. Biochem.* **59**, 1973–1975.
- Fujioka, S., Li, J., Choi, Y.-H., Seto, H., Takatsuto, S., Noguchi, T., Watanabe, T., Kuriyama, H., Yokota, T., Chory, J., and Sakurai, A.** (1997). The *Arabidopsis deetiolated2* mutant is blocked early in brassinosteroid biosynthesis. *Plant Cell* **9**, 1951–1962.
- Gachotte, D., Meens, R., and Benveniste, P.** (1995). An *Arabidopsis* mutant deficient in sterol biosynthesis: Heterologous complementation by *ERG3* encoding a Δ^7 -sterol-C-5-desaturase from yeast. *Plant J.* **8**, 407–416.
- Gachotte, D., Husselstein, T., Bard, M., Lacroute, F., and Benveniste, P.** (1996). Isolation and characterization of an *Arabidopsis thaliana* cDNA encoding a Δ^7 -sterol-C-5-desaturase by functional complementation of a defective yeast mutant. *Plant J.* **9**, 391–398.
- Geber, A., Hitchcock, C.A., Swartz, J.E., Pullen, F.S., Marsden, K.E., Kwon-Chung, K.J., and Bennett, J.E.** (1995). Deletion of the *Candida glabrata* *ERG3* and *ERG11* genes: Effect on cell viability, cell growth, sterol composition, and antifungal susceptibility. *Antimicrob. Agents Chemother.* **39**, 2708–2717.
- Goodwin, T.W.** (1979). Biosynthesis of terpenoids. *Annu. Rev. Plant Physiol.* **30**, 369–404.
- Grebenok, R.J., Galbraith, D.W., and DellaPenna, D.** (1997). Characterization of *Zea mays* endosperm C-24 sterol methyltransferase: One of two types of sterol methyltransferase in higher plants. *Plant Mol. Biol.* **34**, 891–896.
- Grunwald, C.** (1975). Plant sterols. *Annu. Rev. Plant Physiol.* **26**, 209–236.
- Husselstein, T., Gachotte, D., Desprez, T., Bard, M., and Benveniste, P.** (1996). Transformation of *Saccharomyces cerevisiae* with a cDNA encoding a sterol C-methyltransferase from *Arabidopsis thaliana* results in the synthesis of 24-ethyl sterols. *FEBS Lett.* **381**, 87–92.
- Iwasaki, T., and Shibaoka, H.** (1991). Brassinosteroids act as regulators of tracheary-element differentiation in isolated *Zinnia* mesophyll cells. *Plant Cell. Physiol.* **32**, 1007–1014.
- Kauschmann, A., Jessop, A., Koncz, C., Szekeres, M., Willmitzer, L., and Altmann, T.** (1996). Genetic evidence for an essential role of brassinosteroids in plant development. *Plant J.* **9**, 701–713.
- Kim, S.K., Abe, H., Little, C.H.A., and Pharis, R.P.** (1990). Identification of two brassinosteroids from the cambial region of scots pine (*Pinus silvestris*) by gas chromatography–mass spectrometry, after detection using a dwarf rice lamina inclination bioassay. *Plant Physiol.* **94**, 1709–1713.
- Kita, T., Brown, M.S., and Goldstein, J.L.** (1980). Feedback regulation of 3-hydroxy-3-methylglutaryl coenzyme A reductase in livers of mice treated with mevinolin, a competitive inhibitor of the reductase. *J. Clin. Invest.* **66**, 1094–1100.
- Koornneef, M., and Stam, P.** (1992). Genetic analysis. In *Methods in Arabidopsis Research*, C. Koncz, N.-H. Chua, and J. Schell, eds (Singapore: World Scientific Publishing Co.), pp. 83–99.
- Koornneef, M., and van der Veen, J.H.** (1980). Induction and analysis of gibberellin sensitive mutants in *Arabidopsis thaliana* (L.) Heynh. *Theor. Appl. Genet.* **58**, 257–263.
- Koornneef, M., Elgersma, A., Hanhart, C.J., van Loenen-Martinet, E.P., van Rijn, L., and Zeevaart, J.A.D.** (1985). A gibberellin insensitive mutant of *Arabidopsis thaliana*. *Physiol. Plant.* **65**, 33–39.
- Krysan, P.J., Young, J.C., Tax, F., and Sussman, M.R.** (1996). Identification of transferred DNA insertions within *Arabidopsis* genes involved in signal transduction and ion transport. *Proc. Natl. Acad. Sci. USA* **93**, 8145–8150.
- Lecain, E., Chenivesse, X., Spagnoli, R., and Pompon, D.** (1996). Cloning by metabolic interference in yeast and enzymatic characterization of *Arabidopsis thaliana* sterol delta-7-reductase. *J. Biol. Chem.* **271**, 10866–10873.
- Li, J., and Chory, J.** (1997). A putative leucine-rich repeat receptor kinase involved in brassinosteroid signal transduction. *Cell* **90**, 929–938.
- Li, J., Nagpal, P., Vatart, V., McMorris, T.C., and Chory, J.** (1996). A role for brassinosteroids in light-dependent development of *Arabidopsis*. *Science* **272**, 398–401.
- Li, J., Biswas, M.G., Chao, A., Russel, D.W., and Chory, J.** (1997). Conservation of function between mammalian and plant steroid 5 α -reductases. *Proc. Natl. Acad. Sci. USA* **94**, 3554–3559.
- Li, L., and Kaplan, J.** (1996). Characterization of yeast methyl sterol oxidase (*ERG25*) and identification of a human homologue. *J. Biol. Chem.* **271**, 16927–16933.
- Lincoln, C., Britton, J.H., and Estelle, M.** (1990). Growth and development of the *axr1* mutants of *Arabidopsis*. *Plant Cell* **2**, 1071–1080.
- Liu, Y.-G., Mitsukawa, N., Oosumi, T., and Whittier, R.F.** (1995). Efficient isolation and mapping of *Arabidopsis thaliana* T-DNA

- insert junctions by thermal asymmetric interlaced PCR. *Plant J.* **8**, 457–463.
- Mandava, N.B.** (1988). Plant growth-promoting brassinosteroids. *Annu. Rev. Plant Physiol. Plant Mol. Biol.* **39**, 23–52.
- Matsushima, M., Inazawa, J., Takahashi, E., Suzumori, K., and Nakamura, Y.** (1996). Molecular cloning and mapping of a human cDNA (SC5DL) encoding a protein homologous to fungal sterol-C5-desaturase. *Cytogenet. Cell Genet.* **74**, 252–254.
- Mazars, G.-R., Moyret, C., Jeanteur, P., and Theillet, C.-G.** (1991). Direct sequencing by thermal asymmetric PCR. *Nucleic Acids Res.* **19**, 4783.
- Murashige, T., and Skoog, F.** (1962). A revised medium for rapid growth and bioassays with tobacco tissue culture. *Physiol. Plant.* **15**, 473–497.
- Nes, W.R., and McKean, M.L.** (1977). *Biochemistry of Steroids and Other Isopentenoids.* (Baltimore, MD: University Park Press).
- Nomura, T., Nakayama, M., Reid, J.B., Takeuchi, Y., and Yokota, T.** (1997). Blockage of brassinosteroid biosynthesis and sensitivity causes dwarfism in garden pea. *Plant Physiol.* **113**, 31–37.
- Peng, J., and Harberd, N.P.** (1997). Gibberellin deficiency and response mutations suppress the stem elongation phenotype of phytochrome-deficient mutants of *Arabidopsis*. *Plant Physiol.* **113**, 1051–1058.
- Regan, L.** (1993). The design of metal-binding sites in proteins. *Annu. Rev. Biophys. Biomol. Struct.* **22**, 257–281.
- Sasse, J.M.** (1997). Recent progress in brassinosteroid research. *Physiol. Plant.* **100**, 696–701.
- Shanklin, J., Whittle, E., and Fox, B.G.** (1994). Eight histidine residues are catalytically essential in a membrane-associated iron enzyme, stearoyl-CoA desaturase, and are conserved in alkane hydroxylase and xylene monooxygenase. *Biochemistry* **33**, 12787–12794.
- Shi, J., Gonzales, R.A., and Bhattacharyya, M.K.** (1996). Identification and characterization of an *S*-adenosyl-L-methionine: Delta-24-sterol-C-methyltransferase cDNA from soybean. *J. Biol. Chem.* **271**, 9384–9389.
- Smyth, D.R., Bowman, J.L., and Meyerowitz, E.M.** (1990). Early flower development in *Arabidopsis*. *Plant Cell* **2**, 755–767.
- Szekeres, M., Nemeth, K., Koncz-Kalman, Z., Mathur, J., Kauschmann, A., Altmann, T., Redei, G.P., Nagy, F., Schell, J., and Koncz, C.** (1996). Brassinosteroids rescue the deficiency of CYP90, a cytochrome P450 controlling cell elongation and de-etiolation in *Arabidopsis*. *Cell* **85**, 171–182.
- Taguchi, N., Takano, Y., Julmanop, C., Wang, Y., Stock, S., Takemoto, J., and Miyakawa, T.** (1994). Identification and analysis of the *Saccharomyces cerevisiae* *SYR1* gene reveals that ergosterol is involved in the action of syringomycin. *Microbiology* **140**, 353–359.
- Takeno, K., and Pharis, R.P.** (1982). Brassinosteroid-induced bending of the leaf lamina of dwarf rice seedlings: An auxin-mediated phenomenon. *Plant Cell Physiol.* **23**, 1275–1281.
- Taton, M., and Rahier, A.** (1991). Identification of $\Delta^{5,7}$ sterol- Δ^7 reductase in higher plant microsomes. *Biochem. Biophys. Res. Commun.* **181**, 465–473.
- Taton, M., and Rahier, A.** (1996). Plant sterol biosynthesis: Identification and characterization of higher plant Δ^7 -sterol C5(6)-desaturase. *Arch. Biochem. Biophys.* **325**, 279–288.
- Timpte, C.S., Wilson, A.K., and Estelle, M.** (1992). The *axr2-1* mutation of *Arabidopsis thaliana* is a gain-of-function mutation that disrupts an early step in auxin response. *Genetics* **138**, 1239–1249.
- Uwabe, K., Gahara, Y., Yamada, H., Miyake, T., and Kitamura, T.** (1997). Identification and characterization of a novel gene (*neurorep1*) expressed in nerve cells and up-regulated after axotomy. *Neuroscience* **80**, 501–509.
- Yopp, J.H., Mandava, N.B., and Sasse, J.M.** (1981). Brassinolide, a growth-promoting steroidal lactone. I. Activity in selected auxin bioassays. *Physiol. Plant.* **53**, 445–452.

NOTE ADDED IN PROOF

While this article was under review, Husselstein et al. (Husselstein, T., Schaller, H., Gachotte, D., and Benveniste, P. [1999]. Delta7-sterol-C5-desaturase. Molecular characterization and functional expression of wild-type and mutant alleles. *Plant Mol. Biol.*, in press) also showed that a weak allele *ste1-1* contains a substitution mutation in the Δ^7 sterol C-5 desaturase gene, changing a threonine at position 114 to isoleucine.

The Arabidopsis *dwf7/ste1* Mutant Is Defective in the Δ^7 Sterol C-5 Desaturation Step Leading to Brassinosteroid Biosynthesis

Sunghwa Choe, Takahiro Noguchi, Shozo Fujioka, Suguru Takatsuto, Christophe P. Tissier, Brian D. Gregory, Amanda S. Ross, Atsushi Tanaka, Shigeo Yoshida, Frans E. Tax and Kenneth A. Feldmann
Plant Cell 1999;11;207-221
DOI 10.1105/tpc.11.2.207

This information is current as of July 12, 2017

References	This article cites 57 articles, 24 of which can be accessed free at: /content/11/2/207.full.html#ref-list-1
Permissions	https://www.copyright.com/ccc/openurl.do?sid=pd_hw1532298X&issn=1532298X&WT.mc_id=pd_hw1532298X
eTOCs	Sign up for eTOCs at: http://www.plantcell.org/cgi/alerts/ctmain
CiteTrack Alerts	Sign up for CiteTrack Alerts at: http://www.plantcell.org/cgi/alerts/ctmain
Subscription Information	Subscription Information for <i>The Plant Cell</i> and <i>Plant Physiology</i> is available at: http://www.aspb.org/publications/subscriptions.cfm